



The University of
Nottingham

UNITED KINGDOM • CHINA • MALAYSIA

Iqbal, Mudassar and Doherty, Neil and Page, Anna M.L. and Qazi, Saara N.A. and Ajmera, Ishan and Lund, Peter A. and Kypraios, Theodore and Scott, David J. and Hill, Philip J. and Stekel, Dov J. (2017) Reconstructing promoter activity from Lux bioluminescent reporters. *PLoS Computational Biology*, 13 (9). e1005731/1-e1005731/13. ISSN 1553-734X

Access from the University of Nottingham repository:

<http://eprints.nottingham.ac.uk/45487/8/journal.pcbi.1005731.pdf>

Copyright and reuse:

The Nottingham ePrints service makes this work by researchers of the University of Nottingham available open access under the following conditions.

This article is made available under the Creative Commons Attribution licence and may be reused according to the conditions of the licence. For more details see:

<http://creativecommons.org/licenses/by/2.5/>

A note on versions:

The version presented here may differ from the published version or from the version of record. If you wish to cite this item you are advised to consult the publisher's version. Please see the repository url above for details on accessing the published version and note that access may require a subscription.

For more information, please contact eprints@nottingham.ac.uk

RESEARCH ARTICLE

Reconstructing promoter activity from Lux bioluminescent reporters

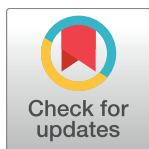
Mudassar Iqbal^{1aa}, Neil Doherty², Anna M. L. Page^{2ab}, Saara N. A. Qazi², Ishan Ajmera³, Peter A. Lund⁴, Theodore Kypraios⁵, David J. Scott², Philip J. Hill², Dov J. Stekel^{1*}

1 Agricultural and Environmental Sciences, School of Biosciences, University of Nottingham, Sutton Bonington Campus, Loughborough, United Kingdom, **2** Food Sciences, School of Biosciences, University of Nottingham, Sutton Bonington Campus, Loughborough, United Kingdom, **3** Plant and Crop Sciences, School of Biosciences, University of Nottingham, Sutton Bonington Campus, Loughborough, United Kingdom, **4** School of Biosciences, University of Birmingham, Birmingham, United Kingdom, **5** School of Mathematical Sciences, University of Nottingham, Nottingham, United Kingdom

^{aa} Current address: Faculty of Biology, Medicine and Health Sciences, University of Manchester, Manchester, United Kingdom

^{ab} Current address: Centre for Biological Sciences, University of Southampton, Southampton, United Kingdom

* dov.stekel@nottingham.ac.uk



OPEN ACCESS

Citation: Iqbal M, Doherty N, Page AML, Qazi SNA, Ajmera I, Lund PA, et al. (2017) Reconstructing promoter activity from Lux bioluminescent reporters. *PLoS Comput Biol* 13(9): e1005731. <https://doi.org/10.1371/journal.pcbi.1005731>

Editor: Jorg Stelling, ETH Zurich, SWITZERLAND

Received: March 28, 2017

Accepted: August 19, 2017

Published: September 18, 2017

Copyright: © 2017 Iqbal et al. This is an open access article distributed under the terms of the [Creative Commons Attribution License](https://creativecommons.org/licenses/by/4.0/), which permits unrestricted use, distribution, and reproduction in any medium, provided the original author and source are credited.

Data Availability Statement: All data and program code are available on Figshare at URL https://figshare.com/projects/Reconstructing_promoter_activity_from_Lux_bioluminescent_reporters/22774. The mathematical model is available at Biomodels with ID MODEL1707200000 (<http://www.ebi.ac.uk/biomodels/>).

Funding: This work was supported by the Biotechnology and Biological Sciences Research Council [grant number BB/I001875/1] (<http://www.bbsrc.ac.uk>); and the Medical Research Council [grant number MR/M012174/1] (<http://www.mrc.ac.uk>) currently funding Mudassar Iqbal. The

Abstract

The bacterial Lux system is used as a gene expression reporter. It is fast, sensitive and non-destructive, enabling high frequency measurements. Originally developed for bacterial cells, it has also been adapted for eukaryotic cells, and can be used for whole cell biosensors, or in real time with live animals without the need for euthanasia. However, correct interpretation of bioluminescent data is limited: the bioluminescence is different from gene expression because of nonlinear molecular and enzyme dynamics of the Lux system. We have developed a computational approach that, for the first time, allows users of Lux assays to infer gene transcription levels from the light output. This approach is based upon a new mathematical model for Lux activity, that includes the actions of LuxAB, LuxEC and Fre, with improved mechanisms for all reactions, as well as synthesis and turn-over of Lux proteins. The model is calibrated with new experimental data for the LuxAB and Fre reactions from *Photobacterium luminescens*—the source of modern Lux reporters—while literature data has been used for LuxEC. Importantly, the data show clear evidence for previously unreported product inhibition for the LuxAB reaction. Model simulations show that predicted bioluminescent profiles can be very different from changes in gene expression, with transient peaks of light output, very similar to light output seen in some experimental data sets. By incorporating the calibrated model into a Bayesian inference scheme, we can reverse engineer promoter activity from the bioluminescence. We show examples where a decrease in bioluminescence would be better interpreted as a switching off of the promoter, or where an increase in bioluminescence would be better interpreted as a longer period of gene expression. This approach could benefit all users of Lux technology.

funders had no role in study design, data collection and analysis, decision to publish, or preparation of the manuscript.

Competing interests: The authors have declared that no competing interests exist.

Author summary

Bioluminescent reporters are used in many areas of biology as fast, sensitive and non-destructive measures of gene expression. They have been developed for bacteria, adapted now for other kinds of organisms, and recently been used for whole cell biosensors, and for real-time live animal models for infection without the need for euthanasia. However, users of Lux technologies rely on the light output being similar to the gene expression they wish to measure. We show that this is not the case. Rather, there is a nonlinear relationship between the two: light output can be misleading and so limits the way that such data can be interpreted. We have developed a new computational method that, for the first time, allows users of Lux reporters to infer accurate gene transcription levels from bioluminescent data. We show examples where a small decrease in light would be better interpreted as promoter being switched off, or where an increase in light would be better interpreted as promoter activity for a longer time.

Introduction

The lux operon contains genes for the bacterial bioluminescent reaction [1, 2]: *luxA* and *luxB* encode the α and β subunits of the heterodimeric bacterial luciferase; *luxC* encodes a 54kDa fatty acid reductase; *luxD* encodes a 33kDa acyl transferase; and *luxE* encodes a 42kDa acylprotein synthetase. These genes, including their order (*luxCDABE*), are conserved in all lux systems of bioluminescent bacteria. An additional gene (*luxF*), with homology to *luxA* and *luxB*, is located between *luxB* and *luxE* in some species. The light emitting reaction, catalysed by the LuxAB complex, involves the oxidation of FMNH₂ and the conversion of a long chain fatty aldehyde (tetradecanal *in vivo*) to its cognate acid, with the emission of blue-green light. LuxC, D and E together form the fatty acid reductase complex, involved in a series of reactions that recycle the fatty acid back to aldehyde. In *E. coli* and other species, Fre has been shown to be the enzyme responsible for flavin reduction back to FMNH₂.

Gene expression can be measured by cloning a promoter of interest upstream of the lux operon, and interpreting the bioluminescence from bacteria containing such constructs as a measure of transcription [3, 4]. This provides a reporter that can measure gene expression at high frequency and with less background noise than other reporters, such as GFP [4, 5], and has found great value in both bacteria [6] and eukaryotes [7], with important recent applications in whole cell biosensors [8], live animal infection models [9, 10] and live tumour infection models [11].

However, this light is an integrated signal of transcription, mRNA half-life, translation and protein turn-over, the bioluminescence reaction kinetics and substrate availability and cycling. As a consequence, absolute transcription activity cannot be directly inferred from the data generated. This is a limitation in the current use of Lux technologies. For example, some studies using Lux reporters have observed fluctuations in light output [12–16], and it is not clear whether these truly reflect promoter activity, or are artefacts of the reporter system.

In this paper we show that detailed mathematical models for bioluminescence can be used to relate bioluminescence to promoter activity. We developed a new model that addresses limitations of previous work [17], whose structure and parameters are informed by new data and new mechanisms. We generated new enzymatic data both for the Fre reaction and for the LuxAB reaction, using *Photorehabdus luminescens* LuxAB that we have purified. An important part of our approach is to fit the models directly to the time series experimental data, which can be thought of as a (partial) factorial experiment with varying concentrations of both FMN

and NADPH. This allows for the simultaneous inference of all parameters in complex kinetic models, which is an advantage over traditional chemical kinetics techniques that only use the maximal velocity.

Results and discussion

New experimental kinetics data for LuxAB and Fre reactions including evidence for product inhibition

The luciferase reaction uses FMNH₂ as an energy source. This is an energetically transient species with a short half-life. *In vivo* it is supplied to the luciferase complex for immediate consumption by the redox activity of the Fre enzyme, which converts NADPH and FMN to FMNH₂ and NADP⁺. We measured the kinetics of the Fre reaction (Fig 1a) by recording the consumption of NADPH (as determined spectrophotometrically) at different starting concentrations of the FMN acceptor component (100 μM, 200 μM and 400 μM); in all cases, the initial NADPH concentration was 200 μM. The initial velocity of the reaction increased with increased FMN, leading to different kinetics in the three curves, with the steady state being reached more rapidly with increased FMN concentration.

For the measurement of luciferase (LuxAB) kinetic reactions, we combined components of the coupled Fre-LuxAB reaction. We measured light output arising from different initial concentrations of FMN: 10 nM, 100 nM, 1 μM, 10 μM and 100 μM (Fig 1a). For all five conditions, there is an initial delay before light is produced, due to a two-step injection method. Following the lag, light is produced, initially rapidly, and then tailing off. A striking feature of these data is that maximum light production increases as FMN concentration is increased from 10 nM to 1 μM, but then decreases again as FMN concentration is increased further. The most likely explanation for this decrease is inhibition of the LuxAB reaction by its product, FMN, which would be competing with FMNH₂ for binding to the LuxAB complex. It cannot be substrate inhibition of Fre by FMN as the kinetics for this reaction increase up to 400 μM (Fig 1a). Product inhibition has not been previously reported and represents a newly discovered element of

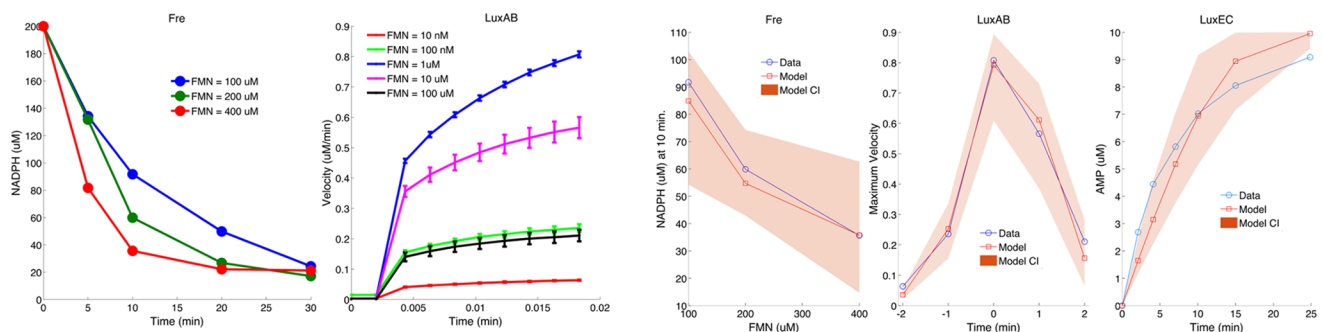


Fig 1. New experimental data and model fits. (a) NADPH time course for three different concentration of FMN for the Fre reaction, and (b) for the LuxAB reaction (means and standard errors from 3 replicates). The concentration values in the above data are obtained from the absorption measurements from the spectrophotometer. The conversion is carried out by relating the concentration (C) to the measured values (A) with the formula $A = K * C$, where K is the proportionality constant and is estimated using initial measurement (A_0) and starting concentration ($C_0 = 200 \mu M$). The velocity of the reaction increases as FMN concentration is increased. Normalised (using max. velocity in the assay) LuxAB reactions velocity time series for different FMN concentrations. The velocity of the reaction increases from the lowest concentrations of FMN, is greatest for FMN concentrations of 1 μM, and decreases for higher concentrations of FMN. This is best explained by product inhibition of the LuxAB reaction through competition between FMN and the substrate FMNH₂. (c) Model fits for Fre, (d) LuxAB, and (e) LuxEC reactions. The model fits to the data are good, showing that kinetic parameters for the reaction rates can be inferred. Summarized data are displayed: for Fre—NADPH concentrations at $t = 10$ min; for LuxAB, the maximal velocity for each FMN concentration; for LuxEC—only the AMP time-course data are shown. The full data and fits for all three reactions are shown in Figures A, B, F and J in S1 Text. Total flavin = 88 μM, O₂ = 550 μM, NADPH = 560 μM, and ATP = 1310.

<https://doi.org/10.1371/journal.pcbi.1005731.g001>

the Lux bioluminescent pathway. Structural studies have shown that both FMN and FMNH₂ can form a complex with LuxAB [18], with only two residues that could act to discriminate between them (see PDB 3fgc), supporting the proposed product inhibition.

New mathematical model for the Lux system with parameters inferred from experimental data

The new mathematical model includes three chemical reactions: the Fre reaction for flavin recycling; the LuxAB reaction for light production; and the LuxEC reaction for aldehyde recycling. It also contains a further equation to describe the turnover dynamics of the Lux proteins:

$$\begin{aligned} \frac{d[\text{FMNH}_2]}{dt} &= v_{\text{Fre}} \text{Fre} - v_{\text{LuxAB}} \text{LuxAB} \\ \frac{d[\text{FMN}]}{dt} &= -v_{\text{Fre}} \text{Fre} + v_{\text{LuxAB}} \text{LuxAB} \\ \frac{d[\text{RCOOH}]}{dt} &= v_{\text{LuxEC}} \text{LuxEC} + v_{\text{LuxAB}} \text{LuxAB} - \tau[\text{RCOOH}] \\ \frac{d[\text{RCHO}]}{dt} &= \rho_0 - v_{\text{LuxAB}} \text{LuxAB} + v_{\text{LuxEC}} \text{LuxEC} - \tau[\text{RCHO}] \\ \frac{dP}{dt} &= T(t) - \gamma_L P \\ [\text{FMNH}_2] + [\text{FMN}] &= F \\ [\text{RCOOH}] + [\text{RCHO}] &= R_0 \end{aligned}$$

It is assumed that the action of LuxD counterbalances the loss of RCOOH and RCHO; thus R_0 is constant and $\rho_0 = \tau R_0$. Control of the bioluminescent reactions is assumed to lie with the most rapidly turned-over protein. This is modelled by setting $P(t)$ to represent all of the Lux proteins and using the same rate of synthesis and turn-over for all proteins. The protein production $T(t)$ encompasses transcription, translation and mRNA degradation and is supplied as a model input; it is assumed that the *lux* mRNA is at quasi steady state. The value of the protein turn-over rate γ_L has been inferred from Lux data as 0.378h^{-1} (Fig 2). Full details for the velocity equations for the terms v_{Fre} , v_{LuxAB} and v_{LuxEC} are provided in S1 Text. New detailed mechanisms have been defined using King and Altman's schematic method [19], with a modification to the v_{LuxAB} velocity term to include the impact of FMNH₂ product inhibition.

We have carried out parameter inference for all three reactions: Fre, LuxAB and LuxEC, using a Markov Chain Monte Carlo (MCMC) approach, as in previous work [20, 21]. The results are posterior distributions for each of the parameters in the model, which describe not only the best fit values for the parameters, but also the degree of uncertainty of the parameter estimates. Because the Fre reaction is also used in the LuxAB experiment, inference for these parameters was carried out in two steps: first we fitted the experimental data from the Fre reaction to produce posterior distribution for these parameters; then we used these posterior distributions as prior distributions for the same parameters in the LuxAB reactions. For the LuxEC reactions, we used published data on steady-state measurements of NADPH, ATP and RCOOH, as well as time-course measurements of AMP formation [1, 22, 23], as shown in Fig 2 (B,F,G, H) of Welham *et al.*[17]. There is good concordance between the model and the data (Fig 1b), with the time course in particular showing substantial improvement ($R^2 = 0.762$) over the model fit previously reported [17] ($R^2 = 0.396$), consistent with improved model mechanism and parameter inference. Detailed fitted curves, MCMC diagnostics and posterior

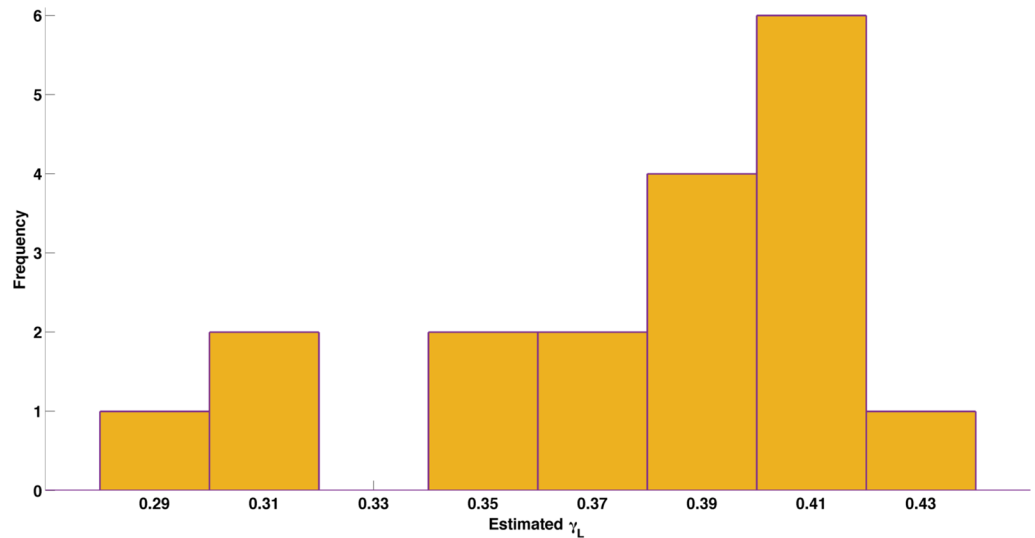


Fig 2. Histogram of inferred Lux protein turnover rates. The histogram shows low variability about a mean value of $0.378h^{-1}$.

<https://doi.org/10.1371/journal.pcbi.1005731.g002>

distributions are shown in Figures B–N in [S1 Text](#) and the inferred parameters are given in Table A in [S1 Text](#).

Model predicts a nonlinear relationship between promoter activity and bioluminescent output

A key finding of this analysis, of particular significance for inferring levels of gene expression with lux reporters, is that there is a nonlinear relationship between promoter activity and light output ([Fig 3](#)). Bioluminescent outputs display qualitative and quantitative behaviours different from the underlying gene expression, so direct interpretation of bioluminescent data can be misleading. Simulations of the model for a switching on of gene expression show that for low levels of expression, bioluminescence appears more gradually with a slight delay, while for higher levels of gene expression there is a transient peak of bioluminescence followed by lower steady state. Simulations for a transient pulse of gene expression also produce bioluminescent outputs that are different from the underlying gene expression. Bioluminescence decreases more slowly than gene expression, and, for higher levels of gene expression, bioluminescence can take several hours to decrease following cessation of gene expression. The decrease in signal is considerably faster than most variants of GFP, which are often stable for more than 24 hours [[5](#), [24](#)], and comparable with engineered unstable GFP variants [[25](#)].

Inference of promoter activity from bioluminescent output

The model can be used to reverse engineer gene expression from bioluminescence, also using an MCMC approach. We have tested this approach on three datasets: the synthetic pulse data set, where the underlying gene expression to be inferred is supplied; data from the *uhpT* promoter in *S. aureus*, with relatively simple light profiles; and data from an acid stress experiment in *E. coli*, with more complicated bioluminescent output, for the promoter of the *safA-ydeO* operon in four strains following exposure to acid: wild-type, a *ydeO* knockout, a *phoP* knockout and a *ydeOphoP* double knock out; both YdeO and PhoP repress this promoter [[15](#)].

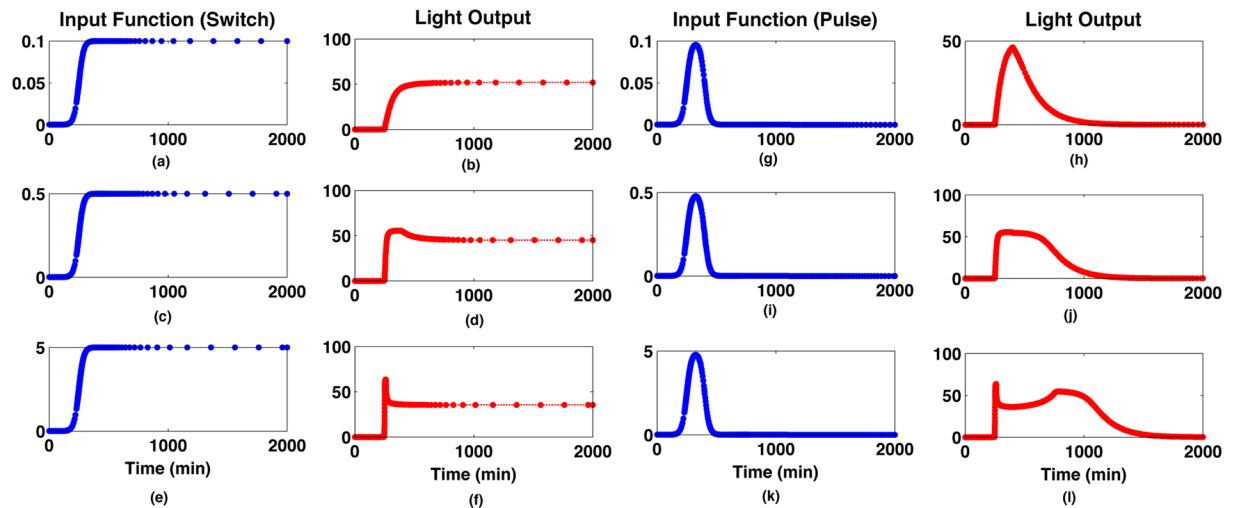


Fig 3. Relationship between promoter activity and light output. Nonlinear relationship between promoter activity and light output for a synthetic pulse or switch of gene expression at different levels. The bioluminescence displays different qualitative and quantitative behaviours from the underlying gene expression. With the switch data, the bioluminescence has slower onset compared with gene expression, and, for high levels of gene expression, shows a transient pulse not present in the gene expression. With the pulse data, the bioluminescence shows much longer persistence than the underlying gene expression. These data show that bioluminescence alone could be a misleading measure of gene expression.

<https://doi.org/10.1371/journal.pcbi.1005731.g003>

The reverse engineering of the synthetic pulse data show accurate reproduction of the supplied input gene expression profile, demonstrating that our method works correctly (Fig 4). For the *uhpT* data (Fig 5a), the inferred promoter activity suggests both earlier gene expression and more rapid switching off of expression than would be apparent from the light output. The most profound difference in interpretation of results based solely on levels of emitted light arise from the acid stress data (Fig 5b). While the inferred gene expression is less smooth than the bioluminescence, it highlights three behaviours not apparent in the bioluminescence itself. First, there is a clear, transient pulse of gene expression following acid stress, lasting only 20 minutes in the WT, 30 minutes in the single knockout strains, and 40 minutes in the double knock-out. In the WT and *ydeO* mutant, gene expression is completely switched off after this pulse, which cannot be seen from the bioluminescence, while in the *phoP* and double mutants, it is not completely switched off. Second, the increase in gene expression in the mutants relative to the WT is much lower than indicated by the bioluminescence, with the increased bioluminescence reflecting increased duration of gene expression as much as increased level. Third, the inferred gene expression appears to show pulses. These reflect the experimental protocol, in which plates were moved between the luminometer and the spectrophotometer every 15 minutes, disturbing the cells. The pulses suggest that the protocol had a more profound impact on cell activity than would be apparent from the light. The peaks of these pulses are more likely to represent gene expression level, indicative of a long term steady state gene expression, also not apparent from the bioluminescence. While the transient gene expression of the *safA-ydeO* promoter is to be expected in the WT and two single mutant strains, the reason for its transience in the double mutant, i.e. in the absence of the two known down-regulators of the promoter, is not known. The promoter is activated by the EvgA response regulator following a drop in pH, and the kinetics of turnover and dephosphorylation of this activator are unknown. They may explain the transient activation of the promoter, or there may be other feedback systems operating. Other known acid responsive regulators such as GadE, GadX and GadW are not responsible, as their deletion has no effect on promoter induction kinetics [15].

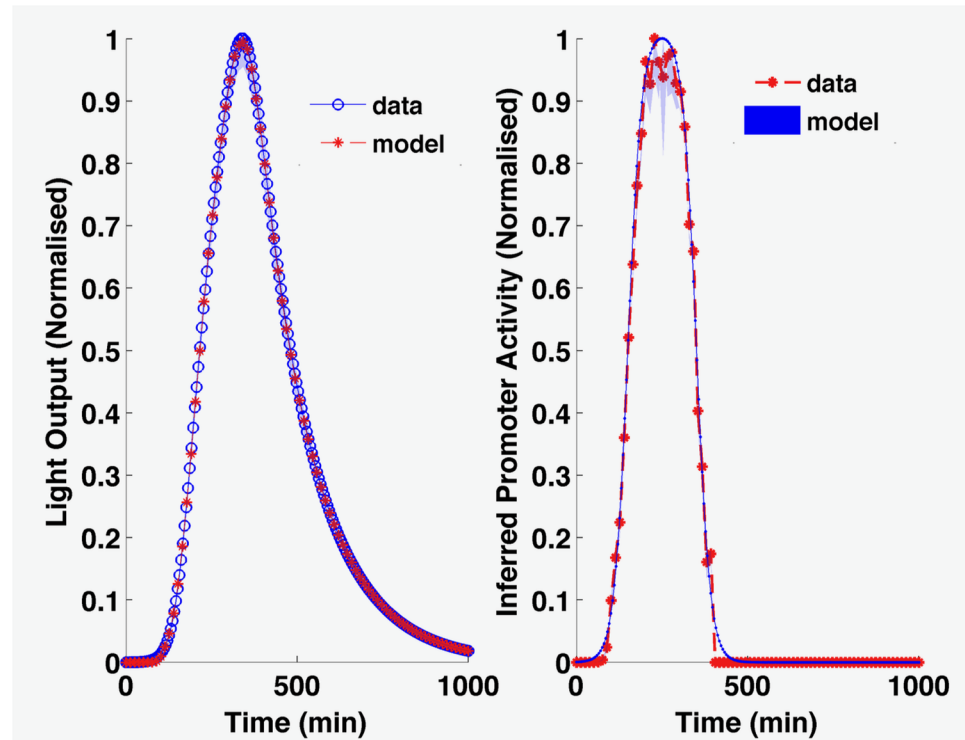


Fig 4. Reverse engineered promoter activity from light output. Here, the promoter inference is for a simulated transient pulse experiment, showing effective and accurate recovery of the known gene expression profile. The shaded areas in the graphs represent 50 simulations resampling from the posterior distribution; they are barely visible because the posterior distribution in this case is very tight.

<https://doi.org/10.1371/journal.pcbi.1005731.g004>

In these cases it is reasonable to associate a reduction of bioluminescence with a reduction of promoter activity. However, the Lux reporter system can also be used to assess loss of cell viability under toxic stress, including to antibiotics [26] or heavy metals [27], with a reduction of bioluminescence associated with cell death. On the other hand, with sub-lethal doses of antimicrobials, the Lux reporter system can still be a useful measure of gene expression, including of antimicrobial resistance genes [20, 28]. Since the model associates changes in bioluminescence to promoter activity, rather than viability, it is important to ensure that there is minimal loss of viability due to experimental conditions, in order that the model output can be correctly interpreted.

Conclusion

We have developed a new mathematical model to relate gene expression to light output in Lux promoter assays, that includes newly discovered experimental evidence for product inhibition of the LuxAB reaction by FMNH₂. The model shows a nonlinear relationship between gene expression and light output. We have used the model to provide a method to infer gene expression from light output that can be generally applied to experiments using Lux reporter assays. We anticipate that this approach could have valuable applications in inferring gene expression levels in a wide range of biological systems where lux reporters can be employed, including both *in vitro* experiments, and to track gene expression in animal models of bacterial infection. Program code to undertake reverse engineering of promoter activity are provided as Matlab and R functions on Figshare.

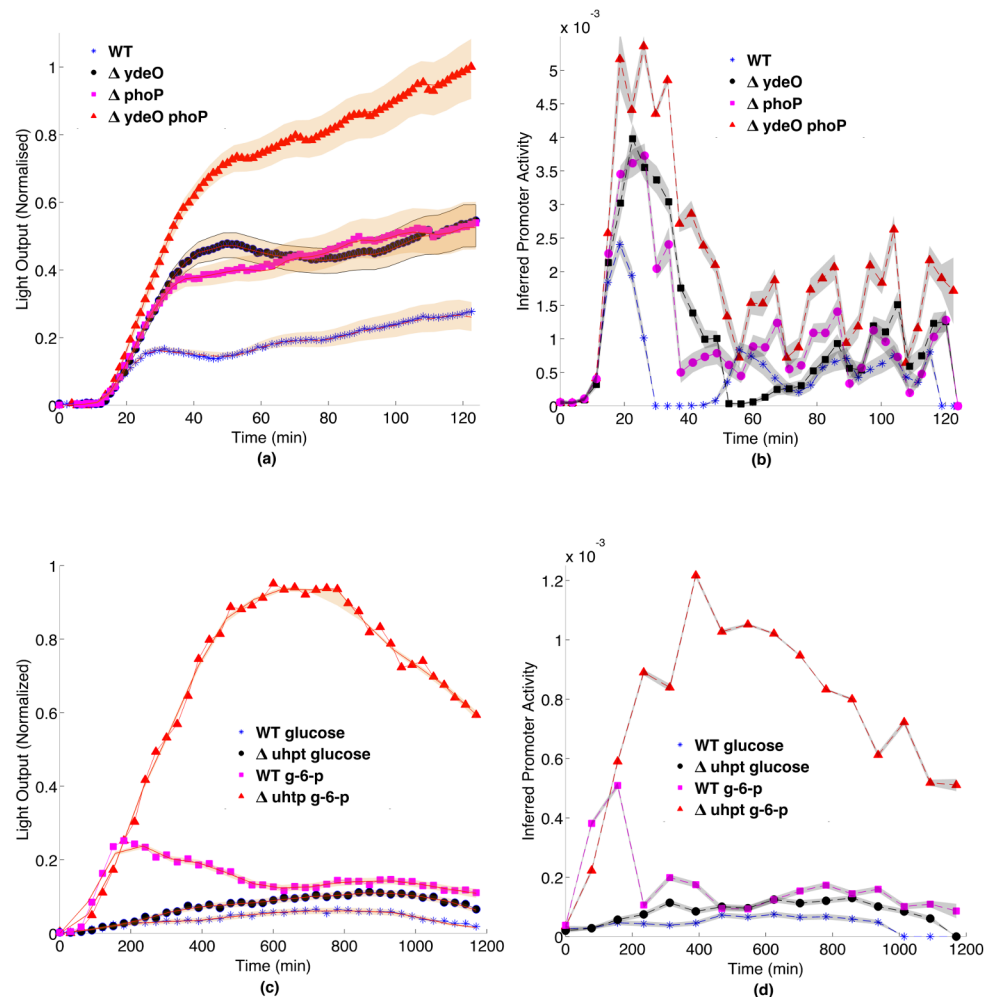


Fig 5. Reverse engineering of promoter activity from experimental data. (a) Bioluminescent data and (b) reverse engineered gene expression from the *safA-ydeO* promoter in *E. coli*. The pattern of gene expression is very different from the light output pattern. In particular, the increased bioluminescence is partly explained by greater duration of gene expression not just level of gene expression; gene expression in the WT and *yodeI* mutant appears to be switched off after induction, which is not apparent in the bioluminescence; and the inferred expression shows pulses which are an artefact of the experimental arrangement, in which plates were moved every 15 minutes between a spectrophotometer and a luminometer, demonstrating that the agitation has an impact upon the cells. The shaded areas in the graphs represent 50 simulations resampling from the posterior distribution. (c) Bioluminescent data and (d) reverse engineered gene expression from data from the *uhpT* promoter in *S. aureus* showing that the peak of gene expression occurs earlier than the light output, and that the duration of gene expression is shorter than would appear from the light output.

<https://doi.org/10.1371/journal.pcbi.1005731.g005>

Materials and methods

Chemicals, media, cloning, bacterial strains

All chemicals were purchased from Sigma-Aldrich unless indicated otherwise, and were of ultrapure quality. Routine cloning steps were carried out using standard molecular biological protocols. Primary clones were selected in LB with Mach I Electrocompetent or chemically *E. coli* obtained from Thermo-Fisher Scientific. Protein expression was carried out using the *E. coli* strain BL21 (DE3) which had been previously transformed with the arabinose inducible plasmid pGRO7, encoding the GroES-GroEL chaperone complex (Takara Inc.).

Autoinduction medium was used for the protein purification steps (Overnight Express Auto-induction system 1—Novagen). See below for further details of the luciferase purification strategy. Antibiotic selection was carried out at the following concentrations: Chloramphenicol— $20\mu\text{gml}^{-1}$, Carbenicillin— $100\mu\text{gml}^{-1}$, Kanamycin— $50\mu\text{gml}^{-1}$.

Measurement of Fre activity

The commercially available Fre/NAD(P)H:FMN-Oxidoreductase of *P. luminescens* was obtained from Roche Diagnostics. The activity of the enzyme was determined using a continuous spectrophotometric rate determination method as follows: NADPH ($200\mu\text{M}$), FMN ($100\text{--}400\mu\text{M}$) and Fre ($5\mu\text{l}$ of a 0.2 unit ml^{-1} preparation per ml final reaction mix) was prepared in 50mM potassium phosphate buffer, pH 7.0. Replicate 1ml samples were prepared in sterile cuvettes, which were mixed by inversion immediately after addition of the enzyme. Fre activity was observed as a function of the loss of NADPH, measured by reduction of its characteristic absorbance value at 340nm . Experiments were conducted over a period of 30 minutes at 22°C . All measurements were performed in triplicate.

Luciferase purification

A co-expression approach was undertaken to purify nascent LuxAB directly from *E. coli* BL21 (DE3). The luciferase genes were amplified from the plasmid pSL1190::luxA2E bearing the *P. luminescens* luciferase operon using the high fidelity polymerase KOD (Merck-Millipore Corp.). *luxA* (Genbank ID AAA276619.1) was amplified using the primer pair: luxAfw 5'-AGCACGCATATGGCGAAATTTGGAAACTTTTTGCTTACA-3' / luxArv 5'-CCGTCGCTCGAGTTAATATAATAGCGAACGTTG-3'. *luxB* (Genbank ID AAA27620.1) was amplified using the primer pair: luxBfw 5'-GAGCACGCATATGGCCAAATTTGGATTGTTCTTCC-3' / luxBrv 5'-CCGTCGCTCGAGTTAGGTATATTTTCATGTGGTACTTC-3'. *luxA* and *luxB* were cloned into pET21b and pET28b respectively, using a *XhoI/NcoI* digest approach. A stop codon was placed in the *luxArv* primer, leaving an N-terminally tagged LuxB and an untagged LuxA in the final expression system. These plasmids were co-transformed into a version of the expression strain which had previously been transformed with the plasmid pGro7, encoding the GroES/GroEL chaperone system. We found that this improved yield of soluble LuxAB. Following overnight growth of the co-expression strain in autoinduction medium containing the appropriate antibiotics and arabinose at 1mgml^{-1} (37°C with shaking), cells were harvested by centrifugation and lysed with the Bugbuster cell lysis reagent with added benzonase and lysozyme according to the manufacturer's instructions (Merck-Millipore Corp.). Clarified lysate was diluted five-fold in wash/bind buffer (20mM tris, 200mM NaCl, pH7.4) containing protease inhibitors (Protease Inhibitor Cocktail—Sigma-Aldrich co.). The resulting preparation was applied to equilibrated Ni^{2+} sepharose columns (HiTrap—GE Healthcare Life Sciences), washed with 100 column volumes wash/bind buffer, and luciferase was eluted in $5 \times 1\text{ml}$ fractions of elution buffer (wash/bind buffer containing 500mM imidazole). Active fractions were assessed using the reconstituted luciferase assay (see section M4) using a Biospace-lab Photon Imager, and combined. The N-terminal his-tag was cleaved from LuxB using 3 units ml^{-1} cleavage-grade thrombin according to the supplier's instructions (Novagen). Cleaved luciferase was buffer exchanged and purified from the released tag and other low molecular weight contaminants such as imidazole using 10kDa nominal molecular weight cut-off centrifugal filter units (Microcon YM10—Sigma-Aldrich Co.). Protein concentration was determined by Bradford assay using a Nanodrop low sample volume UV-Vis Spectrophotometer (Thermo Scientific) using a BSA standard curve.

Reconstitution of coupled luciferase assay and kinetic measurements

Purified luciferase and commercially prepared Fre were combined to form the coupled reaction complex as follows: Reactions were typically carried out in a final volume of 100 μ l containing purified luciferase (typically in the range 1.5–15 μ gml⁻¹), NADPH (200 μ M), FMN (tested over the range 10nM–100 μ M in this study), Fre (0.2 units ml⁻¹) and decanal (0.02%) in 50mM potassium phosphate buffer, pH 7.0. Reactions were carried out at 22°C and monitored in either a Biospacelab Photon Imager or Tecan Genios Pro multimode microplate reader. The kinetic assays were carried out using a Tecan Genios pro fitted with injector capacity as follows; all components other than decanal were combined in a final volume of 50 μ l per well in flat bottomed microtiter plates suitable for bioluminescence measurements. The reactions were initiated by injection of a further 50 μ l phosphate buffer containing 0.04% decanal. Reactions were monitored for 1100 milliseconds. All measurements were performed in triplicate.

Estimation of Lux turnover rates

The promoter of the Universal hexose transporter (*uhpT*) gene was amplified from *S. aureus* and introduced into pUNK1dest along with the Gram-positive GFP-*luxABCDE* operon and the *rrnBT1T2* terminator [29] using a Multisite Gateway LR plus reaction. Transformants were selected on erythromycin and screened for expression of the reporter. This PuhpT-reporter vector was designated pSB3009. *S. aureus* RN4220 [pSB3009] overnight cultures were grown aerobically at 37°C in Tris Minimal Succinate medium (TMS, [30]) supplemented with Erythromycin (5 μ gml⁻¹) for plasmid maintenance. Bacterial pellets were washed once in TMS without sodium succinate (TM) and resuspended in an equal volume of TM. These were diluted 1/50 into fresh TM supplemented with filter sterilized sugars (Glucose or glucose-6-phosphate) supplemented with Erythromycin (5 μ gml⁻¹).

For growth and reporter gene measurements, replicate samples (200 μ l) were placed into the wells of a 96-clear-bottom microtiter plate (Porvair) and incubated at 37°C in a Tecan Genesis Pro microplate reader. Optical density (600nm), fluorescence (485ex/510em) and bioluminescence (RLU) readings were taken at 30 min periods over the course of the experiment.

From the data generated from these experiments, we identified the curves where RLU (light read-outs, arbitrary units) decreases while cells are still in exponential phase (corresponding OD measurements). We estimate the turn-over rate for each such curve (total 18 curves used) by fitting a linear line to the log transformed data. The histogram of estimated values are shown in Fig 2. The linear fits to the log-transformed data for all the 18 curves are shown in Figure O in S1 Text.

Parameter inference

In order to estimate the kinetic parameters for all three reactions, we used a similar Bayesian approach based on Markov Chain Monte Carlo (MCMC), in which a sub-model relevant to each reaction is used along-with corresponding experimental data. We used an adaptive version of Metropolis-Hasting MCMC algorithm with global scaling [31] in order to iteratively sample from the posterior distribution of the kinetic parameters. Our choice of priors and likelihood function is described below.

Unless otherwise specified, we used un-informative exponential priors ($\lambda = 100$) for kinetic parameters, while more informative *gamma* priors (*Gam*(0.9,0.1)) for degradation rates. This reflects our *a priori* knowledge that the kinetic parameters (ratio of kinetic rate constants) are all positive real numbers. For those parameters which are common to the inference in both the Fre and LuxAB models, prior estimates for the LuxAB inference were generated by fitting exponential distributions to the posterior estimates derived from the the Fre inference.

We define the likelihood of the parameters, for any of the models using in Eq 1, assuming homogeneous Gaussian noise. Given the current set of parameter values (θ), we simulate the species of interest (stored in vector Y'), and use the corresponding experimental data in vector Y to give the likelihood function:

$$L(\theta) = \prod_{i=1}^n \left(\frac{\tau}{2\pi}\right)^{\frac{1}{2}} \exp\left(-\frac{\tau}{2}(Y_i - Y'_i)^2\right) \quad (1)$$

A separate Gibbs step is introduced for the sampling of noise precision τ , in case of Fre and LuxEC inference, while for LuxAB data, we estimated the noise variance from the replicates. Details on the derivation of the Gibbs step is provided in S1 Text.

Promoter inference

A Monte Carlo approach was used to infer promoter activity from light readout. The promoter input function is modelled as a series of K heights at fixed positions. A Martingale prior distribution is used [32], so that the prior distribution for each height at point n is an exponential distribution with mean value equal to the current height at the previous point $n-1$. At each step, a point is chosen at random, and a new height is proposed, as described in Green 1995 [33]. The likelihood function uses a Gaussian error model. For all promoter inference, light output curves for a whole experiment must be normalized to the highest light value found in that experiment.

Supporting information

S1 Text. The file S1 Text contains detailed methods of the computational modelling, including reactions mechanisms and related velocity derivations, and details for parameter estimation for all three reactions (Fre, LuxAB, and LuxEC), including relevant sub-models, additional figures for model data fits, diagnostic figures for MCMC methods, details of posterior distributions, and a table of inferred parameters.
(PDF)

Acknowledgments

We thank Tania Pehinec for microbiological technical support.

Author Contributions

Conceptualization: Philip J. Hill, Dov J. Stekel.

Funding acquisition: David J. Scott, Philip J. Hill, Dov J. Stekel.

Investigation: Mudassar Iqbal, Neil Doherty, Anna M. L. Page, Saara N. A. Qazi, Ishan Ajmera.

Methodology: Mudassar Iqbal, Neil Doherty, Theodore Kypraios, David J. Scott, Dov J. Stekel.

Project administration: Dov J. Stekel.

Resources: Peter A. Lund, Philip J. Hill.

Software: Mudassar Iqbal, Dov J. Stekel.

Supervision: David J. Scott, Philip J. Hill, Dov J. Stekel.

Validation: Theodore Kypraios, Philip J. Hill.

Writing – original draft: Mudassar Iqbal, Neil Doherty, Dov J. Stekel.

Writing – review & editing: Peter A. Lund, Theodore Kypraios, Philip J. Hill, Dov J. Stekel.

References

1. Meighan E. Genetics of bacterial bioluminescence. *Annu Rev Genet.* 1994; 28:117–139. <https://doi.org/10.1146/annurev.ge.28.120194.001001>
2. Dunlap P. Biochemistry and genetics of bacterial bioluminescence. *Advances in Biochemical Engineering and Biotechnology.* 2014; 144:37–64.
3. Szittner R, Meighan E. Nucleotide sequence, expression, and properties of luciferase coded by *lux* genes from a terrestrial bacterium. *The Journal of Biological Chemistry.* 1990; 265(27):16581–16587. PMID: 2204626
4. Close D, Xu T, Smartt A, Rogers A, Crossley R, Price S, et al. The evolution of the bacterial luciferase gene cassette (*lux*) as a real-time bioreporter. *Sensors.* 2012; 12:732–752. <https://doi.org/10.3390/s120100732> PMID: 22368493
5. Qazi S, Harrison S, Self T, Williams P, Hill P. Real-time monitoring of intracellular *Staphylococcus aureus* replication. *Journal of Bacteriology.* 2004; 186(4):1065–1077. <https://doi.org/10.1128/JB.186.4.1065-1077.2004> PMID: 14762001
6. Zaslaver A, Mayo A, Rosenberg R, Bashkin P, Sberro H, Tsalyuk M, et al. Just-in-time transcription program in metabolic pathways. *Nature Genetics.* 2004; 36:486–491. <https://doi.org/10.1038/ng1348> PMID: 15107854
7. Close D, Patterson S, Ripp S, Baek S, Sanseverino J, Sayler G. Autonomous bioluminescent expression of the bacterial luciferase gene cassette (*lux*) in a mammalian cell line. *PLoS One.* 2010; 5:e12441. <https://doi.org/10.1371/journal.pone.0012441> PMID: 20805991
8. Brutusco C, Preveral S, Escoffier C, Descamps E, Prudent E, Cayron J, et al. Novel aspects of the acid response network of *Escherichia coli* K-12 are revealed by a study of transcriptional dynamics. *Environ Sci Pollut Res.* 2017; 24:52–65.
9. Bacconi M, Haag A, Torre A, Castagnetti A, Chiarot E, Delany I, et al. A stable luciferase reporter plasmid for in vivo imaging in murine models of *Staphylococcus aureus* infections. *Appl Microbial Biotechnol.* 2016; 100:3197–3206. <https://doi.org/10.1007/s00253-015-7229-2>
10. Shivak D, MacKenzie K, Watson N, Pasternak J, Jones B, Wang Y, et al. A modular, Tn7-based system for making bioluminescent or fluorescent *Salmonella* and *Escherichia coli* strains. *Appl Environ Microbiol.* 2016; 82(16):4931–4943. <https://doi.org/10.1128/AEM.01346-16>
11. Cronin M, Akin A, Francis K, Tangney M. In vivo bioluminescence imaging of intratumoral bacteria. *Methods Mol Biol.* 2016; 1409:69–77. https://doi.org/10.1007/978-1-4939-3515-4_7 PMID: 26846803
12. King J, Digrazia P, Applegate B, Burlage R, Sanseverino J, Dunbar P, et al. Rapid, sensitive bioluminescent reporter technology for naphthalene exposure and biodegradation. *Science.* 1990; 249:778–781. <https://doi.org/10.1126/science.249.4970.778> PMID: 17756791
13. Zanzotto A, Boccazzi P, Gorret N, Van Dyk T, Sinskey A, Jensen J. *In situ* measurement of bioluminescence and fluorescence in an integrated microbioreactor. *Biotechnology and Bioengineering.* 2006; 93:40–47. <https://doi.org/10.1002/bit.20708> PMID: 16187336
14. Qazi S, Middleton B, Muharram S, Cockayne A, Hill P, O'Shea P, et al. N-acylhomoserine lactones antagonize virulence gene expression and quorum sensing in *Staphylococcus aureus*. *Infection and Immunity.* 2006; 74(2):910–919. <https://doi.org/10.1128/IAI.74.2.910-919.2006> PMID: 16428734
15. Burton N, Johnson M, Antczak P, Robinson A, Lund P. Novel aspects of the acid response network of *Escherichia coli* K-12 are revealed by a study of transcriptional dynamics. *Journal of Molecular Biology.* 2010; 401(5):726–742. <https://doi.org/10.1016/j.jmb.2010.06.054> PMID: 20603130
16. Jia K, Eltzov E, Marks R, Ionescu R. Bioluminescence enhancement through an added washing protocol enabling a greater sensitivity to carbofuran toxicity. *Ecotoxicology and Environmental Safety.* 2013; 96:61–66. <https://doi.org/10.1016/j.ecoenv.2013.06.013> PMID: 23867093
17. Welham P, Stekel D. Mathematical model of the Lux luminescence system in the terrestrial bacterium *Photobacterium luminescens*. *Molecular Biosystems.* 2009; 5:68–76. <https://doi.org/10.1039/B812094C> PMID: 19081933
18. Campbell Z, Weichsel A, Montfort W, Baldwin T. Crystal structure of the bacterial luciferase/flavin complex provides insight into the function of the beta subunit. *Biochemistry.* 2009; 48:6085–6094. <https://doi.org/10.1021/bi900003t> PMID: 19435287

19. King E, Altman C. A schematic method of deriving the rate laws for enzyme-catalyzed reactions. *J Phys Chem*. 1956; 60(10):1375–1378. <https://doi.org/10.1021/j150544a010>
20. Takahashi H, Oshima T, Hobman J, Doherty N, Clayton S, Iqbal M, et al. The dynamic balance of import and export of zinc in *Escherichia coli* suggests a heterogeneous population response to stress. *Journal of the Royal Society Interface*. 2015; 12(106). <https://doi.org/10.1098/rsif.2015.0069>
21. Fletcher S, Iqbal M, Jabbari S, Stekel D, Rappoport J. Analysis of occludin trafficking, demonstrating continuous endocytosis, degradation, recycling and biosynthetic secretory trafficking. *PLoS ONE*. 2014; 9(11):e111176. <https://doi.org/10.1371/journal.pone.0111176> PMID: 25422932
22. Rodriguez A, Riendeau D, Meighan E. Purification of the acyl coenzyme A reductase component from a complex responsible for the reduction of fatty acids in bioluminescent bacteria. Properties and acyl-transferase activity. *The Journal of Biological Chemistry*. 1983; 258(8):233–5237.
23. Rodriguez A, Nabi I, Meighan E. ATP turnover by the fatty acid reductase complex of *Photobacterium phosphoreum*. *Canadian Journal of Biochemistry and Cell Biology*. 1985; 63(10):1106–1111.
24. Qazi S, Council E, Morrissey J, Rees C, Cockayne A, Winzer K, et al. *agr* expression precedes escape of internalised *Staphylococcus aureus* from the host endosome. *Infection and Immunity*. 2001; 69(11):7074–7082. <https://doi.org/10.1128/IAI.69.11.7074-7082.2001> PMID: 11598083
25. Allen M, Wilgus J, Chewning C, Saylor G, Simpson M. A destabilized bacterial luciferase for dynamic gene expression studies. *Systems and Synthetic Biology*. 2007; 1:3–9. <https://doi.org/10.1007/s11693-006-9001-5> PMID: 19003433
26. Vocat A, Hartkoorn R, Lechartier B, Zhang M, Dhar N, Cole S, et al. Bioluminescence for assessing drug potency against nonreplicating *Mycobacterium tuberculosis*. *Antimicrobial Agents and Chemotherapy*. 2015; 59:4012–41019. <https://doi.org/10.1128/AAC.00528-15> PMID: 25896710
27. Ivask A, Rolova T, Kahru A. A suite of recombinant luminescent bacterial strains for the quantification of bioavailable heavy metals and toxicity testing. *BMC Biotechnology*. 2009; 9:41. <https://doi.org/10.1186/1472-6750-9-41> PMID: 19426479
28. Melamed S, Lalush C, Elad T, Yagur-Kroll S, Belkin S, Pedahzur R. A bacterial reporter panel for the detection and classification of antibiotic substances. *Molecular Biotechnology*. 2012; 5:536–548.
29. Pehinec T, Qazi S, Gaddipati S, Salisbury V, Rees C, Hill P. Construction and evaluation of multisite recombinatorial (gateway) cloning vectors for Gram-positive bacteria. *BMC Molecular Biology*. 2007; 8:80. <https://doi.org/10.1186/1471-2199-8-80> PMID: 17880697
30. Sebulsky M, Hohnstein D, Hunter M, DE H. Identification and characterization of a membrane permease involved in iron-hydroxamate transport in *Staphylococcus aureus*. *Journal of Bacteriology*. 2000; 182(16):4394–4400. <https://doi.org/10.1128/JB.182.16.4394-4400.2000> PMID: 10913070
31. Andrieu C, Thoms J. A tutorial on adaptive MCMC. *Statistics and Computing*. 2008; 18(4):343–373. <https://doi.org/10.1007/s11222-008-9110-y>
32. Arjas E, Gasbarra D. Nonparametric Bayesian inference from right censored survival data, using the Gibbs sampler. *Statistica sinica*. 1994; 4:505–524.
33. Green P. Reversible jumble Markov chain Monte Carlo computation and Bayesian model determination. *Biometrika*. 1995; 82(4):711–732. <https://doi.org/10.1093/biomet/82.4.711>